

Reactions of Nitrogen Oxides with Heme Models. Characterization of NO and NO₂ Dissociation from Fe(TPP)(NO₂)(NO) by Flash Photolysis and Rapid Dilution Techniques: Fe(TPP)(NO₂) as an Unstable Intermediate

Mark D. Lim,[†] Ivan M. Lorkovic,^{*,†} Katrin Wedeking,[†] Andrew W. Zanella,[‡]
Carmen F. Works,[†] Steve M. Massick,[†] and Peter C. Ford^{*,†}

Contribution from the Department of Chemistry and Biochemistry, University of California,
Santa Barbara, California 93106, and Joint Science Department, Claremont Colleges,
Claremont, California 91711-5916

Received May 6, 2002

Abstract: Described are studies directed toward elucidating the controversial chemistry relating to the solution phase reactions of nitric oxide with the iron(II) porphyrin complex Fe(TPP)(NO) (**1**, TPP = *meso*-tetraphenylporphinato²⁻). The only reaction observable with clean NO is the formation of the diamagnetic dinitrosyl species Fe(TPP)(NO)₂ (**2**), and this is seen only at low temperatures ($K_1 < 3 \text{ M}^{-1}$ at ambient temperature). However, **1** does readily react reversibly with N₂O₃ in the presence of excess NO to give the nitro nitrosyl complex Fe(TPP)(NO₂)(NO) (**3**), suggesting that previous claims that **1** promotes NO disproportionation to give **3** may have been compromised by traces of air in the nitric oxide sources. It is also noted that **3** undergoes reversible loss of NO to give the elusive nitro species Fe(TPP)(NO₂) (**4**), which has been implicated as a powerful oxygen atom transfer agent in reactions with various substrates. Furthermore, in the presence of excess NO₂, the latter undergoes oxidation to the stable nitrate analogue Fe(TPP)(NO₃) (**5**). Owing to such reactivity of Fe(TPP)(NO₂), flash photolysis and stopped-flow kinetics rather than static techniques were necessary for the accurate measurement of dissociation equilibria characteristic of Fe(TPP)(NO₂)(NO) in 298 K toluene solution. Flash photolysis of **3** resulted in competitive NO₂ and NO dissociation to give Fe(TPP)(NO) and Fe(TPP)(NO₂), respectively. The rate constant for the reaction of **1** with N₂O₃ to generate Fe(TPP)(NO₂)(NO) was determined to be $1.8 \times 10^6 \text{ M}^{-1} \text{ s}^{-1}$, and that for the NO reaction with **4** was similarly determined to be $4.2 \times 10^5 \text{ M}^{-1} \text{ s}^{-1}$. Stopped-flow rapid dilution techniques were used to determine the rate constant for NO dissociation from **3** as 2.6 s^{-1} . The rapid dilution experiments also demonstrated that Fe(TPP)(NO₂) readily undergoes further oxidation to give Fe(TPP)(NO₃). The mechanistic implications of these observations are discussed, and it is suggested that NO₂ liberated spontaneously from Fe(P)(NO₂) may play a role in an important oxidative process involving this elusive species.

Introduction

Given continuing elucidation of the biological functions of nitric oxide (nitrogen monoxide),¹ the interactions of NO and other NO_x species with relevant metal centers have become increasingly important to model. Of particular interest is nitrogen oxide speciation in the presence of ferri- and ferro-hemes in aerobic aqueous and hydrophobic media given the roles played by hemes in the biological synthesis and bioregulatory actions of NO.

The iron(II) heme model Fe(TPP) forms a stable nitrosyl complex Fe(TPP)(NO) (**1**, TPP = *meso*-tetraphenylporphinato²⁻)

via addition of NO.² However, there have been conflicting reports²⁻⁷ describing products from the further reaction of **1** with excess NO in solution. A recent communication^{6a} from this laboratory demonstrated the equilibrium formation of the diamagnetic dinitrosyl species Fe(TPP)(NO)₂ (**2**) (eq 1), which can be observed at low temperature using proton NMR techniques. The interaction is relatively weak ($K_1 < 3 \text{ M}^{-1}$ at 298 K), so there is little evidence for the formation of **2** in ambient temperature solutions. EPR evidence consistent with eq 1 was described in a much earlier report by Wayland and Olson.²

* To whom correspondence should be addressed. E-mail: ford@chem.ucsb.edu.

[†] University of California, Santa Barbara.

[‡] Claremont Colleges.

(1) (a) *Nitric Oxide, Biology, and Pathobiology*; Ignarro, L. J., Ed.; Academic Press: San Diego, 2000. (b) Feelisch, M., Stamler, J. S., Eds. *Methods in Nitric Oxide Research*; Wiley: Chichester, U.K., 1996 and references therein.

(2) (a) Wayland, B. B.; Olson, L. W. *J. Am. Chem. Soc.* **1974**, *96*, 6037–6041. (b) Scheidt, W. R.; Frisse, M. E. *J. Am. Chem. Soc.* **1975**, *97*, 17–21.

(3) Langon, D.; Kadish, K. M. *J. Am. Chem. Soc.* **1983**, *105*, 5610–5617.

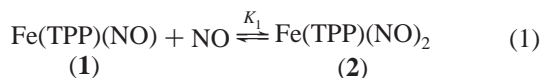
(4) Yoshimura, T. *Inorg. Chim. Acta* **1984**, *83*, 17–21.

(5) Ellison, M. K.; Schulz, C. E.; Scheidt, W. R. *Inorg. Chem.* **1999**, *38*, 100–108.

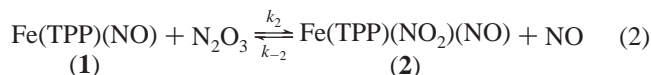
(6) (a) Lorkovic, I. M.; Ford, P. C. *J. Am. Chem. Soc.* **2000**, *122*, 6516–6517.

(b) Lorkovic, I. M.; Ford, P. C. *Inorg. Chem.* **2000**, *39*, 632–633.

(7) Lin, R.; Farmer, P. J. *J. Am. Chem. Soc.* **2001**, *123*, 1143–1150.

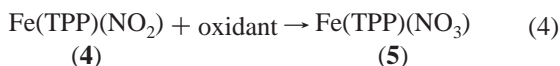
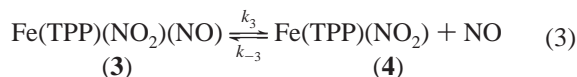


Other workers⁷ have subsequently disputed this observation and argued that NO disproportionation is promoted by **1** to give the nitro nitrosyl complex Fe(TPP)(NO₂)(NO) (**3**). Indeed, this reaction finds analogy in NO reactions with ruthenium(II) and osmium(II) porphyrins⁸ as well as with certain non-heme iron complexes.⁹ While we, in contrast, did not find NO disproportionation to result from mixing solutions of **1** with *clean* NO at ambient temperature,^{6a} we have demonstrated that Fe(TPP)(NO) reacts readily with N₂O₃ in the presence of excess NO to give the nitro nitrosyl complex Fe(TPP)(NO₂)(NO) (**3**).^{6b}



These observations suggest that claims that **1** promotes NO disproportionation in ambient temperature solutions may be compromised by the presence of traces of air or other NO_x in the nitric oxide sources.

We have also reported^{6b} that, upon removal of the NO atmosphere from a solution containing **3**, this species undergoes further reaction (eq 3), NO dissociation to give the nitro (or nitrito) complex Fe(TPP)(NO₂) (**4**).⁵ However, as will be described below, **4** is unstable and undergoes further oxidation (eq 4) to the nitrato complex Fe(TPP)(NO₃) (**5**), which has an optical spectrum very similar to that of **4**.¹⁰



There have been multiple reports in the literature describing the reactivity of ferric porphyrin complexes of the nitrite ion, NO₂⁻. For example, Scheidt and co-workers^{11c} characterized Fe(TpivPP)(NO₂) as a high spin complex (β -pyrrole ¹H NMR: $\delta = 75$ ppm) intermediate formed during addition of [K(18-crown-6)][NO₂] to Fe(TpivPP)(H₂O)(CF₃SO₃) (TpivPP = $\alpha,\alpha,\alpha,\alpha$ -tetrakis(2-pivalamidophenyl)porphinato²⁻). The same species was isolated by Richter-Addo et al.¹² as the aerobic oxidation product of Fe(TpivPP)(NO) in the presence of pyridine. Subsequently, Scheidt et al. used EPR to characterize **4** (formed by BF₃ abstraction of NO₂⁻ from the stable anionic complex Fe(TPP)(NO₂)₂⁻) and noted its propensity to dispropo-

portionate to **1** plus **5**.^{11c} A similar nitro complex Fe(OEP)(NO₂) was implicated by Castro¹³ as an intermediate in the oxidation of alkenes (to form epoxides) by mixtures of Fe(OEP)-Cl and nitrite salts dissolved in *N*-methylpyrrolidinone solution with 1% acetic acid. Presumably, this involves oxygen atom transfer from N-coordinated nitro ligand to give the oxidized substrate plus the stable Fe(II) nitrosyl complex Fe(OEP)(NO).

Clearly, the system that is generated from a solution of Fe(TPP)(NO) in equilibrium with gaseous NO plus small amounts of air or other NO_x as impurities represents a complex mixture of reactive species and dynamic equilibria. The present work is directed toward elucidating such interactions with the goals of better understanding reactions of higher nitrogen oxides with heme proteins and of reconciling seemingly conflicting observations regarding these deceptively complex and reactive systems. In the interest of resolving the latter ambiguities, we describe here quantitative investigations of the reaction equilibria and kinetics that characterize the above mixture. The present report will present additional documentation regarding reactions 1 and 2 as well as a kinetics study of the reactive species Fe(TPP)(NO₂) formed from **3** by two methods, flash photolysis or by stopped-flow rapid dilution.

Experimental Section

Toluene was distilled from CaH₂. Spectrochemical grade toluene was prepared by washing with sulfuric acid and neutralizing with NaOH to remove residual thiophene, followed by distillation from sodium. Deuterated solvents for NMR studies (Cambridge Isotope Laboratories, Inc.) were used without further purification. Nitric oxide (99%, Aire Liquide) was purified by passage through a stainless steel column containing Ascarite II (Thomas Scientific), attached via O-ring seal (Viton) to a greaseless vacuum line.¹⁴ Solutions of known [NO] were prepared manometrically by vacuum transfer techniques with flasks of known volume. UV-vis measurements were conducted on an HP 8452A Diode Array spectrophotometer using custom-made cuvettes fused to a flask equipped with a high-vacuum stopcock and coldfinger for conducting anaerobic measurements. ¹H NMR measurements were conducted on a Varian 400 MHz instrument.

Fe(TPP)(NO₂)(NO) solutions were prepared by adding measured aliquots of air to toluene solutions of Fe(P)(NO) and NO. Sample solutions for flash photolysis studies were prepared from **2** (10–20 μ M) in CHCl₃ or toluene under various NO pressures or under NO with aliquots of air to prepare N₂O₃ solutions.

Flash Photolysis Experiments. The flash apparatus has been described previously.¹⁵ This consisted of a frequency tripled Nd:YAG, Continuum NY-61 excitation source (355 nm, 10 ns fwhm, 20 mJ/pulse, 2 Hz), and the decays of transient absorbance or bleach at various wavelengths were monitored with monochromatic probe light. The probe beam was focused into the sample (at a right angle to the excitation beam), through a double grating monochromator (SPEX

(8) (a) Miranda, K. M.; Bu, X.; Lorkovic, I. M.; Ford, P. C. *Inorg. Chem.* **1997**, *36*, 4838–4848. (b) Kadish, K. M.; Adamian, V. A.; Caemelbecke, E. V.; Tan, Z.; Tagliatesta, P.; Bianco, P.; Boschi, T.; Yi, G.-B.; Khan, M. A.; Richter-Addo, G. B. *Inorg. Chem.* **1996**, *35*, 1343–1348. (c) Bohle, D. S.; Goodson, P. A.; Smith, B. D. *Polyhedron* **1996**, *15*, 3147–3150. (d) Lorkovic, I. M.; Ford, P. C. *Inorg. Chem.* **1999**, *38*, 1467–1473. (e) Lorkovic, I. M.; Leal, F. I.; Ford, P. C.; Richter-Addo, G. B., manuscript in preparation.

(9) Franz, K. J.; Lippard, S. J. *J. Am. Chem. Soc.* **1999**, *121*, 10504.

(10) The Soret band maxima in toluene solution for the various porphyrin complexes discussed in this manuscript are: Fe(TPP)(NO) (**1**), 406 nm ($\epsilon = 1 \times 10^5 \text{ M}^{-1} \text{ cm}^{-1}$); Fe(TPP)(NO₂)(NO) (**2**), 432 nm ($\epsilon = 1.8 \times 10^5 \text{ M}^{-1} \text{ cm}^{-1}$); Fe(TPP)(NO₂) (**3**), 412 nm ($\epsilon = 1.1 \times 10^5 \text{ M}^{-1} \text{ cm}^{-1}$); Fe(TPP)(NO₃) (**4**), 412 nm ($\epsilon = 1.1 \times 10^5 \text{ M}^{-1} \text{ cm}^{-1}$).

(11) (a) Nasri, H.; Goodwin, J. A.; Scheidt, W. R. *Inorg. Chem.* **1990**, *29*, 185–191. (b) Finnegan, M. G.; Lappin, A. G.; Scheidt, W. R. *Inorg. Chem.* **1990**, *29*, 181–185. (c) Munro, O. Q.; Scheidt, W. R. *Inorg. Chem.* **1998**, *37*, 2308–2316.

(12) Cheng, L.; Powell, D. R.; Khan, M. A.; Richter-Addo, G. B. *Chem. Commun.* **2000**, *23*, 2301.

(13) (a) O'Shea, S. K.; Wang, W.; Wade, R. S.; Castro, C. E. *J. Org. Chem.* **1996**, *61*, 6388–6395. (b) Castro, C. E. *J. Am. Chem. Soc.* **1996**, *118*, 3984–5398.

(14) For the preparation of the dinitrosyl complex **2**, where traces of N₂O₃ were especially damaging, more extensive procedures were adopted. NO was purified by passing through an Ascarite scrubber, then through an activated silica (80–100 mesh) packed column (5 ft, 3/8" stainless steel tubing coil) at -78 °C. The latter procedure removed N₂O and any residual NO₂ and N₂O₃. (Warning: At -78 °C, considerable NO absorbs in the column, and precaution should be taken for the controlled NO release when the system warms to room temperature.) Solutions were prepared and transferred to cells with gastight syringes inside an inert atmosphere "drybox". Materials in contact with NO solutions (septa, stopcocks, and plungers) were deaerated by storage in the drybox for at least 18 h prior to solution exposure.

(15) Lorkovic, I. M.; Miranda, K. M.; Lee, B.; Bernhard, S.; Schoonover, J. R.; Ford, P. C. *J. Am. Chem. Soc.* **1998**, *120*, 11674–11683.

Model 1680), and onto a photomultiplier tube (RCA IP28 for 400–600 nm, RCA 8852/230 for 600–800 nm). The temporal response (50 shot averages) was recorded on a digital oscilloscope (Tektronix TDS 540) linked to a desktop computer. Plots of intensity versus time were converted to absorbance, and the curves were fit to single or double exponentials using Igor (Wavemetrics) software.

Stopped-Flow Experiments. These were performed on an Applied Photophysics SX-17MV stopped-flow spectrometer using standard asymmetric sequential mixing modes. The sample (A) and flush (F) drive syringes were changed from the stock 2.5 mL syringe to 250 μ L (Hamilton Salt Line #1725 AD-SL) syringes. Solutions were loaded into drive syringes from the solution flask via gastight syringes (Hamilton Gastight #1010 SL) equipped with removable needles and exit valves, permitting evacuation of the drive syringes and transfer volume prior to loading. Rapid dilution of Fe(TPP)(NO₂)(NO) solutions was accomplished by asymmetric mixing of a solution of Fe(TPP)(NO₂)(NO), NO, and N₂O₃ (1.5, 3–12, and 1–6 mM, respectively) in toluene from a 250 μ L syringe, with toluene from a 2.5 mL (11-fold dilution) syringe into an aging loop. After 25 ms, the solution was driven by toluene in a 250 μ L syringe together with a 2.5 mL syringe into the second mixing chamber (overall 121-fold dilution), observation cell, and stop syringe.¹⁶ Dilution reproducibility was found to be within 5% using an unreactive absorbing sample of Fe(TPP)Cl (Midcentury Chemicals) and dilution in toluene.

Preparation of 4. An authentic sample of Fe(TPP)(NO₃) [¹H NMR: C₆D₆, 78.4 ppm (β -pyrrole)] was prepared by treatment of the μ -oxo dimer, [Fe(TPP)]₂O (Soret, λ_{max} = 410 nm; Q-band, λ_{max} = 572 nm in CH₂Cl₂), with dilute aqueous HNO₃.¹⁷

Results and Discussion

Reaction of Fe(TPP)(NO) with NO and with N₂O₃. As we described in a preliminary communication,^{6a} the reaction of clean NO with **1** in toluene solution gave the dinitrosyl complex Fe(TPP)(NO)₂ (eq 1) at low temperature. This is further demonstrated by the reversible changes in the optical and IR spectra of the equilibrium mixture of **1** and **2** under NO upon lowering *T* (Figure 1). The proton NMR spectra show **2** to be diamagnetic, and variable *T* studies of NMR line broadening and shifts allowed for the calculation of the equilibrium constant *K*₁ as 23 M⁻¹ at 253 K and 3.1 \times 10³ M⁻¹ at 179 K (ΔH° = -6.7 \pm 0.8 kcal mol⁻¹ and ΔS° = -21 \pm 4 cal mol⁻¹ K⁻¹) for eq 1.^{6a} Accordingly, *K*₁ < 3 M⁻¹ at ambient temperature. The IR spectrum of **2** in 173 K methylcyclohexane solution prepared under a 1:1 mixture of ¹⁵NO and ¹⁴NO gave three ν_{NO} peaks with a 1:2:1 intensity ratio. This pattern is interpreted as corresponding to the unlabeled, singly labeled, and doubly labeled forms of Fe(P)(NO)₂ suggesting a trans, centrosymmetric structure for **2**.

Under ambient temperature conditions (or lower), the spectra of toluene solutions of **1** (Soret band, λ_{max} 406 nm) under an atmosphere of clean NO gave no indication of the nitro nitrosyl complex Fe(TPP)(NO₂)(NO), a species that is structurally⁵ and spectrally¹⁸ well characterized. However, as we have reported,^{6b} introduction of small quantities of air leads to the rapid appearance of **3** (λ_{max} 432 nm) as the result of NO autoxidation to NO₂ (principally N₂O₃ under excess NO). The equilibrium

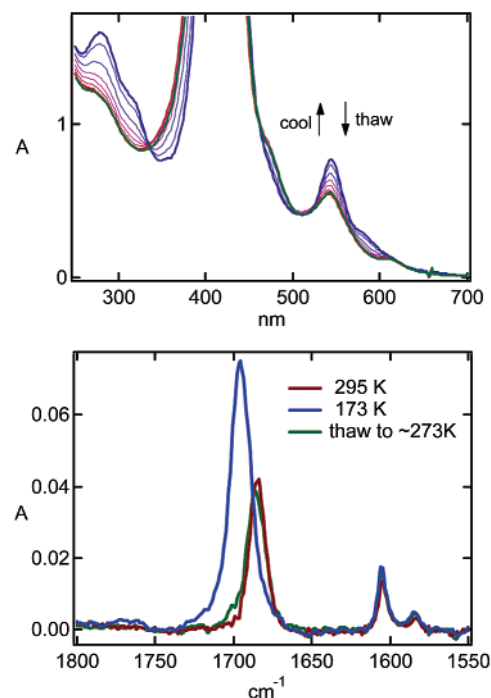


Figure 1. Top: Optical spectra changes upon cooling a solution of Fe(TPP)(NO) in the presence of 8 mM NO in CHCl₃ to 173 K, followed by warming to \sim 273 K. Bottom: Analogous experiment probing IR spectra changes upon cooling a methylcyclohexane solution of Fe(TmTP)(NO) plus NO (8 mM) to 173 K, followed by warming to \sim 273 K. (The TmTP complex was used in this case to improve solubility in methylcyclohexane, TmTP = tetra-(*m*-toluyl)porphinato²⁻.)

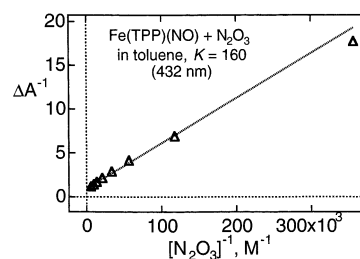


Figure 2. Equilibrium constant measurement for the formation of **3** from **1** and N₂O₃ in toluene at 22 \pm 1 $^\circ$ C (eq 2), obtained by addition of air aliquots (5, 10, 15, 20, 30, 40, 50, 100 μ L) to a 117 mL cell containing **1** (8 μ M) in toluene (25 mL) and NO (500 Torr, 8 mM). The equilibrium constant shown was obtained by fitting the plot of ΔA^{-1} (432 nm) vs $[N_2O_3]^{-1}$ to a line (weighted by ΔA). The N₂O₃ generated by NO autoxidation is assumed to be entirely in the solution. The slope and intercept of this plot are equal to $K_2^{-1}\gamma^{-1}[\text{NO}]$, and γ^{-1} , respectively, where γ is $(\epsilon_2 - \epsilon_1)C_0$, and C_0 is the total concentration of Fe(TPP) species. The intercept divided by the slope gives $K_2[\text{NO}]^{-1}$, and multiplication by $[\text{NO}]$ gives K_2 .

constant *K*₂ was evaluated from the spectral changes as microliter aliquots of air were introduced into a dilute toluene solution of **1** (8 μ M) and NO (8 mM) (Figure 1). Stepwise addition of O₂ led to decreased absorbance at 406 nm and increases at 432 nm (λ_{max} for **3**) and increased absorbance at 306 nm due to the buildup of N₂O₃ (ϵ = 2 \times 10³ M⁻¹ cm⁻¹), and these spectral changes values were used to determine *K*₂ = 160 \pm 20 by standard methods¹⁹ (Figure 2). Analogous studies here have investigated the equilibrium constant for reaction of N₂O₃ with other Fe(P)(NO) complexes (P = various porphyrins) and have noted *K*₅ to range from 1.0 for P = tetrakis-

(16) It should be noted that, upon dilution, N₂O₃ is expected to dissociate to NO and NO₂ ($> 10^4$ s⁻¹) and that, therefore, [NO] after dilution should be regarded as a lower limit.

(17) (a) Phillippi, M. A.; Baenziger, N.; Goff, H. M. *Inorg. Chem.* **1981**, *20*, 3904–3911. (b) Notably, the species formed when **4** was dissolved in CDCl₃ was Fe(TPP)Cl, while in toluene the sample remained 4. (c) Reed, C. A.; Guiset, F. *J. Am. Chem. Soc.* **1996**, *118*, 3281–3282.

(18) Settin, M. F.; Fanning, J. C. *Inorg. Chem.* **1988**, *27*, 1431–1435.

(19) Hoshino, M.; Ozawa, K.; Seki, H.; Ford, P. C. *J. Am. Chem. Soc.* **1993**, *115*, 9568–9575.

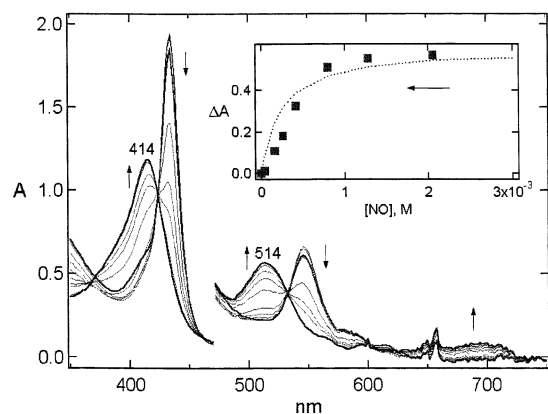
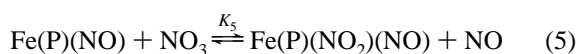


Figure 3. Attempted steady-state equilibrium (K_3) measurement for eq 3, performed by sequential controlled diminution of [NO] in a solution originally containing **3** and excess NO. Inset: Plot of the change in absorbance vs [NO], monitored at 432 nm. The dashed line demonstrates the expected Lineweaver–Burke behavior for a K_2 of 5×10^{-4} M. The poor agreement to the fit suggests that the model does not describe the system adequately under these conditions.

(pentafluorophenyl)porphine to 400 for P = OEP.²⁰ The consistent trend is for NO₂ binding to be more favorable for the more electron-donating porphyrins.



While Fe(TPP)(NO₂)(NO) proved to be relatively stable under high [NO] (>4 mM) and well defined [N₂O₃], it decomposed when [NO] was lowered. For example, ¹H NMR analysis showed the final product in CHCl₃ to be Fe(TPP)Cl, (82.2 ppm) while in toluene it was Fe(TPP)(NO₃)(δ 78.46 ppm) (**5**). The identities of these products were corroborated by comparing the δ values of the paramagnetically shifted β -pyrrole protons to authentic samples of Fe(TPP)Cl and of **5**.¹⁷

In another experiment, a concentrated toluene solution of Fe(TPP)(NO₂)(NO) was prepared under a NO/N₂O₃ atmosphere; then the system was rapidly evacuated so that the solvent and all volatile NO_x species were removed. The solid residue was then redissolved in benzene-*d*₆ under inert atmosphere and transferred to an airtight NMR tube for observation. The spectrum showed a resonance of 76.55 ppm, which was concluded to be the β -pyrrole of **4**. Over the course of an hour, this peak disappeared and gave way to one at 78.46 ppm, matching the spectrum of a sample of **5** prepared by literature methods.¹⁷

Steady-State Experiments To Measure K_3 . Initial attempts to determine the equilibrium constant for NO dissociation from Fe(TPP)(NO₂)(NO) to give Fe(TPP)(NO₂) (eq 3) employed steady-state techniques, that is, controlled removal of NO from the headspace gas over a solution of **3**. The resulting changes in the optical spectra are shown in Figure 3. Although isosbestic points were apparent, the spectral changes were not completely reversible upon reintroduction of NO to original pressures. Furthermore, the spectral changes did not give a good fit to the [NO] dependence expected for simple equilibrium between **3** and **4** (represented by the dashed line in the inset of Figure 3, which is a fit to an apparent dissociation constant of 5×10^{-4} M). Although the K_3 thus estimated was close to that reported

(20) Lorkovic, I. M.; Lim, M. D.; Wedeking, K.; Ford, P. C., manuscript in preparation.

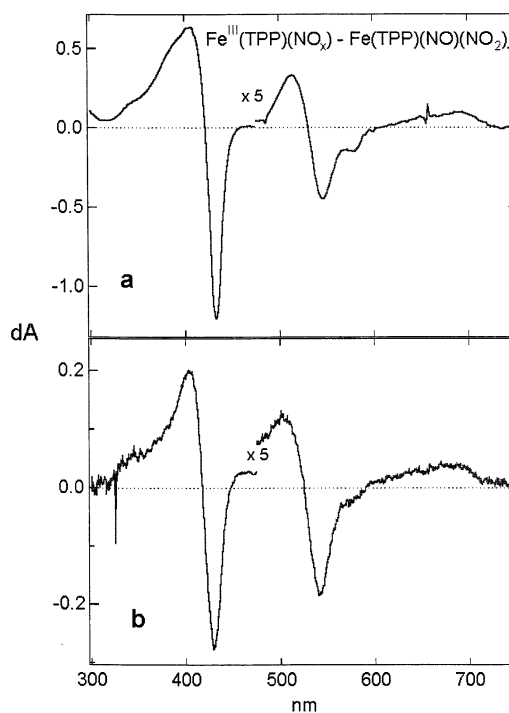


Figure 4. (a) Difference spectra obtained by subtraction of the spectrum of **3** from the spectrum of Fe(P)(NO_x) (obtained upon removal of NO from a solution of **3**). (b) Transient difference spectrum obtained using a CCD detector in the 355 nm laser flash photolysis of a CHCl₃ solution of **3**.

for the analogous reaction of Fe(TpivPP)(NO₂)(NO) ($K = 8 \times 10^{-4}$ M),²¹ the poor fit to Lineweaver–Burke behavior¹⁹ and the irreversibility of the reaction indicated that there may be a secondary process which converts **4** to a spectroscopically similar species which binds NO differently.

Flash Photolysis of **3.** Flash excitation of metalloporphyrins under excess NO results in photolabilization of the nitrosyl complex.²² The subsequent exponential relaxation gives k_{obs} values equal to $k_{\text{on}}[\text{NO}] + k_{\text{off}}$, and the respective rate constants can be extracted from a plot of k_{obs} versus [NO]. The equilibrium constant for NO dissociation can then be calculated from the ratio $k_{\text{off}}/k_{\text{on}}$.

Flash photolysis of **3** in both toluene and CHCl₃ (298 K) led to transient difference spectra (recorded with a CCD detector) such as Figure 4. These difference spectra are nearly identical to the difference spectrum between **3** and the product (or products) formed when excess NO and other volatiles were quickly removed from a solution of the former.²³ The temporal absorbance at 680 nm (characteristic of the NO loss photoproduct, presumably **4**) decayed exponentially to give k_{obs} values that proved to be a linear function of [NO] (Figure 5). The slope of this plot was taken to be the second-order rate constant, $k_{-3} = (4.2 \pm 0.5) \times 10^5 \text{ M}^{-1} \text{ s}^{-1}$. Notably, the k_{obs} values measured at 680 nm were independent of the concentration of N₂O₃, consistent with the view that the process observed at this wavelength is indeed the reaction of **4** with NO to give **3**.

In contrast, the temporal absorbance changes monitored at 432 nm showed a strong bleach in absorbance followed by a

(21) Frangione, M.; Port, J.; Baldiwala, M.; Judd, A.; Galley, J.; DeVega, M.; Linna, K.; Caron, L.; Anderson, E.; Goodwin, J. A. *Inorg. Chem.* **1997**, *36*, 1904–1911.

(22) Laverman, L. E.; Ford, P. C. *J. Am. Chem. Soc.* **2001**, *123*, 11614–11622.

(23) The spectral changes in Figure 1 are consistent with the formation of any high spin Fe(TPP)X, where X may be NO₂⁻, NO₃⁻, or halides, all of which have nearly identical electronic spectra (ref 9).

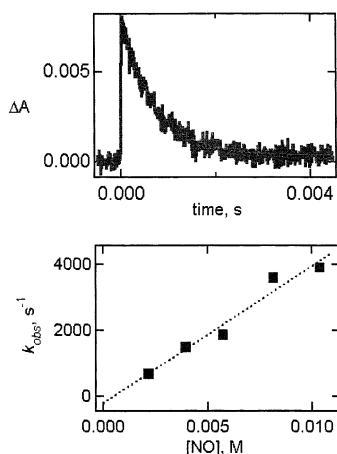


Figure 5. Flash photolysis of solutions of Fe(TPP)(NO₂)(NO) in toluene solution, under varying concentrations of NO and monitored at 680 nm. Top: Transient absorbance trace at 680 nm upon flash photolysis of **3** (25 μM). [NO] = 2.5 mM, [N₂O₃] = 100 μM; the fit to an exponential function ($k_{\text{obs}} = 1.45 \times 10^3 \text{ s}^{-1}$) is shown by the dashed line. Bottom: Plot of k_{obs} vs [NO] for spectral changes at 680 nm, representing reformation of **3** from **4** (slope = $k_{\text{NO}} = (4.2 \pm 0.5) \times 10^3 \text{ M}^{-1} \text{ s}^{-1}$).

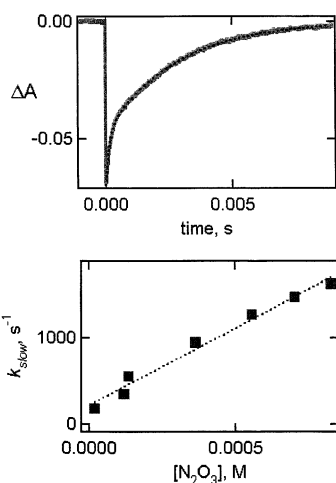
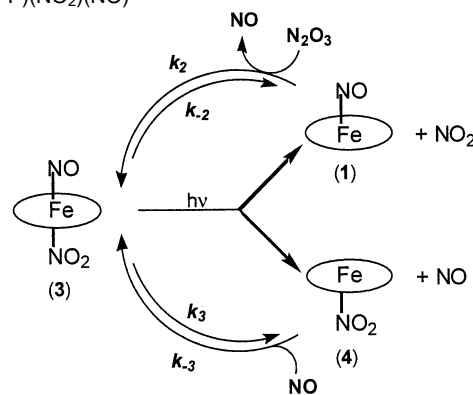


Figure 6. Flash photolysis of Fe(TPP)(NO₂)(NO) in toluene solution, under varying concentrations of NO and monitored at 432 nm. Top: Transient absorbance decay after 355 nm photolysis of **3** (10 μM, [NO] = 8 mM, [N₂O₃] = 100 μM), showing evidence of two processes leading to reformation of **3**. The dotted line shows the fit to a double exponential decay with two first-order rate constants, k_{fast} ($7.7 \times 10^3 \text{ s}^{-1}$) and k_{slow} ($3.5 \times 10^2 \text{ s}^{-1}$). Note: The rate constant for the faster process (k_{fast}) was the same as the k_{obs} determined under these conditions when monitored at 680 nm (see Figure 3). Bottom: Plot of k_{slow} vs [N₂O₃]. This was assigned to the reformation of **3** from photogenerated **1** (slope = $k_{\text{N}_2\text{O}_3} = (1.8 \pm 0.2) \times 10^6 \text{ M}^{-1} \text{ s}^{-1}$).

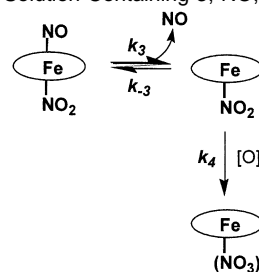
biexponential return to the parent compound (Figure 6). The rate constant of the faster process (k_{fast}) was the same as the k_{obs} for the single exponential found when monitoring at 680 nm under the same conditions. The slower process gave rate constants k_{slow} that proved to be linearly dependent on the concentration of N₂O₃ (Figure 6 (bottom)). Thus, this process was assigned to reaction of **1** with N₂O₃ to re-form **3**. The slope of the k_{obs} versus [N₂O₃] plot gave the second-order rate constant, $k_2 = (1.8 \pm 0.2) \times 10^6 \text{ M}^{-1} \text{ s}^{-1}$.

Thus, the flash photolysis of **3** leads to the competitive dissociation of both NO and NO₂, and the spectroscopic properties of the products (**1** and **4**) are sufficiently distinct to study the respective relaxation processes (Scheme 1). Given that

Scheme 1. Reactions of Species Generated by Flash Photolysis of Fe(TPP)(NO₂)(NO)



Scheme 2. Processes Observed Subsequent to Stopped-Flow Rapid Dilution of a Solution Containing **3**, NO, and N₂O₃



$K_2 = k_2/k_{-2}$, use of the previously measured $K_2(160)^2$ allowed for the calculation of k_{-2} as $1.1 \times 10^4 \text{ M}^{-1} \text{ s}^{-1}$.

Stopped-Flow Experiments. Although, in principle, the [NO] = 0 intercept of Figure 5 (bottom) gives the rate constant for NO dissociation from **3** (k_3), the intercept is too small to measure reliably in this manner. Instead, stopped-flow experiments were attempted. Toluene solutions of **3** were prepared in situ by stopped-flow mixing of solutions of **1** with dilute solutions of NO containing small concentrations of N₂O₃. Under these conditions, measured values of k_3 were extremely variable. Qualitative observations suggested that k_3 increased with increasing [N₂O₃] at constant [NO], offering the possibility that NO is abstracted from **3** by NO₂, although some other mechanism may be responsible. Therefore, it appeared to be necessary to minimize both [NO] and [N₂O₃] to characterize unimolecular NO dissociation rates. Because both NO and N₂O₃ are required for the long-term stability of **3**, rapid high dilution techniques were pursued.

Concentrated toluene solutions of **3**, NO, and N₂O₃ were prepared and rapidly mixed in two sequential 11-fold dilutions into pure toluene (121-fold overall). The rapid dilution resulted in a nonequilibrium concentration of **3**, which then decayed via NO dissociation to form **4** and subsequently to form **5** (Scheme 2).

The results of these experiments are shown in Figure 7. The curves in Figure 7 (top) show the absorbance growth at 412 nm resulting from the rapid dilution of a solution containing **3** (~1.5 mM), NO (4.6 mM), and N₂O₃ (~3 mM). The absorbance changes were bimodal; there was a rapid absorbance increase complete within the first 0.5 s and then a slower increase typically complete within 2 min. The rapid step can be attributed to the rapid re-equilibration between **3** and **4** at the new lower [NO], while the slower process represents subsequent oxidation of **4** to the spectrally similar **5**.²³ The magnitude of the

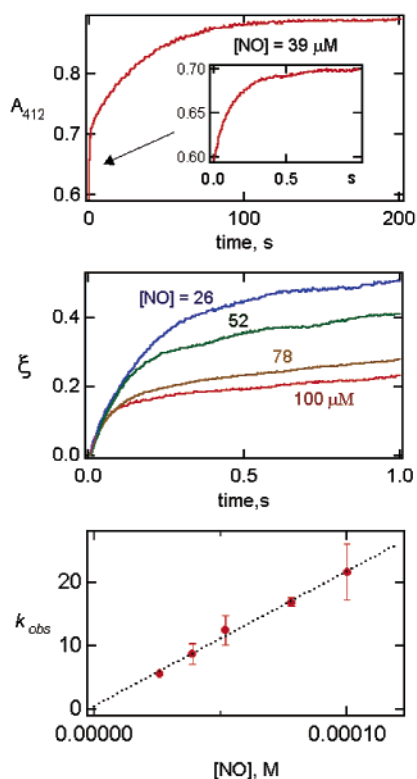


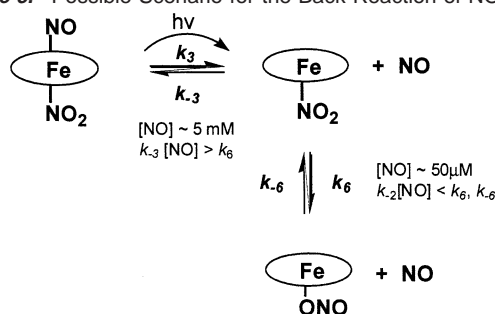
Figure 7. Temporal absorbance changes upon 121-fold rapid dilution of toluene solutions of Fe(TPP)(NO₂)(NO), NO (3–12 mM), and N₂O₃ (~3 mM). Top: Absorbance at 412 nm showing initial rapid rise representing rapid equilibration between **3** and **4** (inset), followed by a longer term absorbance rise representing complete conversion of **3** and **4** to **5**. Middle: Time dependence of extent of reaction (ξ) of K_3 using averaged spectral change data at 432 nm (fall) and 412 nm (rise). Extent of reaction was obtained by normalizing the rapid absorbance change to the total absorbance change over the longer term. Linear fit of the first 25 ms of the normalized data gives an [NO] independent initial rate of $k_{\text{off}} = 2.6 \pm 4 \text{ s}^{-1}$. Bottom: Rate of approach to initial equilibrium as a function of [NO]; a linear fit gives a slope corresponding to $k_{-3} = (2.2 \pm 5) \times 10^5 \text{ M}^{-1} \text{ s}^{-1}$.

absorbance change during the fast stage was much less than would be expected for complete conversion of **3** to **4** ($\Delta A_i = 0.10$ vs $\Delta A_{\text{tot}} \approx 0.3$ expected at 412 nm for $[\mathbf{3}] = 12 \mu\text{M}$). However, the two processes *together* did account for complete conversion of **3**. The spectral characteristics of the products from the fast and slow processes were similar and corresponded to the spectral change seen in Figure 4. On this basis, the ratio of initial absorbance change (ΔA_i) to total absorbance change (ΔA_{tot}) for the overall process may be used to quantify $K_3 \approx 2.4 \times 10^{-5} \text{ M}$ (see Supporting Figure S-1). Notably, this is about 20-fold smaller than that estimated from the Lineweaver–Burke plot described in Figure 3.

In this context, a plot of k_i versus [NO] should be linear according to the relationship $k_i = k_3 + k_{-3}[\text{NO}]$ for a system approaching equilibrium. To approach the y-intercept (k_3) as closely as possible, it was desirable to prepare solutions of **3** with minimal [NO], although solutions having [NO] < 4 mM underwent slow decomposition. However, the *relative* contributions of the fast and slow components, that is, $\Delta A_i/\Delta A_{\text{tot}}$, may still be used to represent the extent of reaction for the fast process, even for cases when partial conversion of **3** to **5** had occurred prior to dilution and observation.

Figure 7 (middle) shows that as [NO] is increased, k_{obs} for the rapid process increases, while the initial extent of reaction ($\xi = \Delta A_i/\Delta A_{\text{tot}}$) due to the equilibration between **3** and **4**

Scheme 3. Possible Scenario for the Back Reaction of NO with **4**



decreases. The initial rate of change gave the best measurement of k_3 , as follows. If $\xi(t)$ is taken to represent the time-dependent extent of the reaction of **3**, and rapid approach to K_3 is observed, then the following relationship holds

$$\xi_{\text{int}} = \frac{[\mathbf{4}]}{[\mathbf{3}] + [\mathbf{4}]} = \frac{K_3 + [\text{NO}]^{-1}}{K_3} = k_3(k_3 + k_{-3}[\text{NO}])^{-1} \quad (6)$$

where ξ_{int} is defined as the extent of reaction at the conclusion of the rapid process, before evolution of the slower process. The approach to this equilibrium may also be written in terms of ξ and the time derivative to give

$$\frac{d}{dt}[\xi(t)] = \xi_{\text{int}} \{1 - e^{-(k_3 + k_{-3}[\text{NO}])t}\} = k_3 e^{-(k_3 + k_{-3}[\text{NO}])t} \Rightarrow k_3$$

for

$$t \ll (k_3 + k_{-3}[\text{NO}])^{-1} \quad (7)$$

In other words, the initial rate of change in extent of reaction is simply k_3 , for any given [NO]. This is illustrated by Figure 7(middle), which gives $k_3 = 2.6 \pm 0.4 \text{ s}^{-1}$. The full course of this initial equilibration monitored at 412 and 432 nm may also be fit to an exponential to obtain k_{obs} . Values of k_{obs} plotted versus [NO] are linear (Figure 7 (bottom)) in accord with a second-order reaction of **4** with NO to regenerate **3**. Accordingly, the slope is $k_{-3} = (2.2 \pm 0.5) \times 10^5 \text{ M}^{-1} \text{ s}^{-1}$.²⁴ Notably, this value is an upper limit because the [NO] values used did not account for NO released owing to N₂O₃ dissociation, although the correction would be <25%. In principle, the intercept gives k_3 , but the initial rate method (Figure 7 (middle)) is much more accurate in this case.

Comparison of the k_{-3} values measured by the flash photolysis and rapid dilution techniques for the “on” reaction of NO with **3** shows that these are not in exact agreement. The disagreement may have its origin in the different techniques employed. Under the high [NO] (~5 mM) used in flash photolysis experiments, the k_{obs} values fall in the range 10^3 – 10^4 s^{-1} ($=k_{-3}[\text{NO}]$, Figure 6b), much higher than the k_{obs} 's (~10 s⁻¹) observed in the rapid dilution studies where [NO] is very low (~50 μM). One might speculate that on the longer time scale of the stopped-flow experiments, there is equilibration between linkage isomers of **3** (Scheme 3). If the nitro isomer reacts more rapidly with NO, the depleted concentration of that species would be reflected in lower apparent values of k_{-3} .

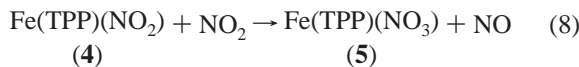
(24) Notably, this value is an upper limit because the [NO] values used did not account for NO released owing to N₂O₃ dissociation, although the correction would be <25%.

Table 1. Summary of Equilibrium and Rate Constants (298 K) Described in This Work^a

reaction	k_f	k_b	K_i
1 + NO \rightleftharpoons 2			$<3 \text{ M}^{-1 b}$
1 + N ₂ O ₃ \rightleftharpoons 3 + NO	$1.8 \times 10^6 \text{ M}^{-1} \text{ s}^{-1 c}$	$1.1 \times 10^4 \text{ M}^{-1} \text{ s}^{-1 c}$	160^b
3 \rightleftharpoons 4 + NO	$2.6 \text{ s}^{-1 d}$	$4.2 \times 10^5 \text{ M}^{-1} \text{ s}^{-1 c}$	$1.2 \times 10^{-5} \text{ M}$
4 + NO ₂ \rightleftharpoons 5 + NO	$\sim 1 \times 10^3 \text{ M}^{-1} \text{ s}^{-1 d}$	$2.2 \times 10^5 \text{ M}^{-1} \text{ s}^{-1 d}$	$6.2 \times 10^{-6} \text{ M}$

^a **1** = Fe(TPP)(NO), **2** = Fe(TPP)(NO)₂, **3** = Fe(TPP)(NO₂)(NO), **4** = Fe(TPP)(NO₂), **5** = Fe(TPP)(NO₃); k_f is the forward rate constant, k_b is the back rate constant, and K_i is the equilibrium constant (k_f/k_b) determined for the reaction shown. Error limits are described in the text. ^b From static spectroscopic measurements. ^c From flash photolysis experiments. ^d From stopped-flow rapid dilution experiments.

The slower process observed in the stopped-flow dilution experiments is the conversion of the **3** plus **4** mixture to the nitrate complex **5**. The rate of this transformation is dependent on [N₂O₃]. Although concentrated ($>100 \mu\text{M}$) solutions of **3** have been reported to disproportionate (to **1** plus **5**),¹⁰ this process occurred over the course of hours. Thus, it is likely that the **3** \rightarrow **5** transformation seen here involves oxidation by low concentrations of NO₂/N₂O₃ or mostly NO₂ in dilute solution (eq 8). Despite significant experimental uncertainty under these conditions (e.g., $k_{\text{slow}} = 0.02 \pm 0.01$ for [NO₂/N₂O₃] = 20 μM), the rate constant k_4 (Scheme 2) can be estimated as $\sim 10^3 \text{ M}^{-1} \text{ s}^{-1}$.



These observations are in agreement with IR spectral studies by Kurtikyan et al.²⁵ of the reactions between films of sublimed Fe(TPP) and NO_x gases in a high-vacuum system. Reaction with NO₂ leads to the nitrate complex **5** (ν_{NO_3} 1526, 1271 cm^{-1}) as the stable product, presumably via oxidation of the intermediate **4** by NO₂. On the other hand, when Fe(TPP) films were exposed to a mixture of NO and NO₂ (i.e., N₂O₃), the IR spectrum characteristic of **3** ($\nu_{\text{NO}} = 1877 \text{ cm}^{-1}$; $\nu_{\text{NO}_2} = 1464, 1300 \text{ cm}^{-1}$) was immediately apparent.

Summary

The present study was initiated in part to elucidate the disproportionation of NO reported to be promoted by reaction with Fe(TPP)(NO) (**1**) and which parallels studies in this laboratory with analogous ruthenium and osmium complexes. However, such disproportionation does not occur readily with **1** under NO at ambient temperature. There are no obvious spectral changes upon exposing solutions of **1** to clean NO, and analogous studies elsewhere with films of solid **1** gave a similar result.²⁵ In lower temperature solutions, the optical, IR, and ¹H NMR spectral properties all point to the reversible formation of a dinitrosyl complex Fe(TPP)(NO)₂ (**2**) in agreement with an earlier interpretation of ESR spectral changes for a similar solution.^{2a} On the other hand, **1** does react readily with N₂O₃ (generated from traces of O₂ in excess NO), so we conclude

that **3** is not formed by the direct reaction of **1** with NO and that reports to the contrary may have been compromised by trace impurities of higher NO_x species. We have not detected the presence of an ambient temperature intermediate attributed⁷ to NO addition to the nitrosyl nitrogen of **1**. While it has been argued⁷ that our conditions are sufficiently different to prevent such an observation, we doubt that the difference lies in the proposal⁷ that these systems are subject to inhibition by protonic impurities. Kutikyan et al. have found the IR frequency shifts claimed as evidence of this interaction in thin films are more likely the result of annealing the films.^{25b}

When N₂O₃ (NO₂) is introduced to the stable solutions of **1** under clean NO, the nitro nitrosyl complex Fe(TPP)(NO₂)(NO) (**3**) is the result. This is relatively stable in the presence of excess NO and N₂O₃, but when the concentrations are lowered by stopped-flow dilution, NO dissociates from **3** to form Fe(TPP)(NO₂), which undergoes further reaction to give the nitrate complex **5**. The similarities of the optical spectra of **4** and **5** may have misled others with regard to the relative stability of the former. In the present studies, it is clear that **4** undergoes fairly rapid oxidation by NO₂/N₂O₃ to **5**. Because this reaction also occurs in the solid state,²⁵ we suggest that NO₂ dissociation followed by oxygen atom transfer may be one source of such oxidations.

Table 1 summarizes the rate constants elucidating the present system. While the chemical transformations characterized here are in media far from biological conditions, such processes are likely to be general to the reactivity of heme enzyme models with nitric oxides in a hydrophobic environment. The quantitative studies reported provide a baseline of reactivity patterns to be expected in the absence of specific effects induced by the protein. Furthermore, these studies emphasize the importance of characterizing not only the reactions of NO with biologically relevant targets but also the need to elucidate the reactivities of other free and coordinated NO_x species.

Acknowledgment. The authors thank the National Science Foundation (C.F.W.), the ACS Petroleum Research Fund (M.D.L., I.M.L., A.A.Z.), and the U.S. Department of Energy (S.M.M.) for financial support of this work. We thank Dr. T. S. Kurtikyan of the Armenian Research Institute of Applied Chemistry for bringing ref 25 to our attention.

Supporting Information Available: Plot of [NO] versus 1/ξ (PDF). This material is available free of charge via the Internet at <http://pubs.acs.org>.

JA020653A

(25) (a) Kurtikyan, T. S.; Stepanyan, T. G.; Akopyan, M. E. *Russ. J. Coord. Chem.* **1999**, *25*, 721–725. (b) These workers (ref 25c) find ν_{NO} changes in these films associated with a phase change from amorphous (1677 cm^{-1}) to ordered film (1697 cm^{-1}), induced by annealing the film at $\sim 80 \text{ }^\circ\text{C}$, and then recooling. Similar changes have been attributed to H₂O binding,⁷ but in these high-vacuum experiments the water activity should be very low. (c) Personal communication from T. S. Kurtikyan.